Journal of Electronic Materials manuscript No.
(will be inserted by the editor)

Molecular Beam Epitaxy and p-type Doping of ZnMgSTe Quaternary Alloys

K. Ichino · K. Sahashi · N. Nanba · T. Nakashima · Y. Tomita · K. Akaiwa · T. Abe

Received: date / Accepted: date

Abstract ZnS-based ZnMgSTe quaternary alloy layers have been grown by molecular beam epitaxy. The bandgap of ZnMgSTe has been estimated from the reflectance spectra, and it was found that it increases with increasing Mg content, while it decreases with increasing Te content. Nitrogen acceptor doping to $Zn_{1-x}Mg_xS_{1-y}Te_y$ layers has also been investigated. The layers with Te content $y > 0.1$ were found to be p-type, and the layer with larger the Te content exhibits lower resistivity. From these

K. Ichino · K. Sahashi · N. Nanba · T. Nakashima · Y. Tomita · K. Akaiwa · T. Abe

Department of Information and Electronics, Tottori University, 4-101 Koyama-minami, Tottori, 680-8552, Japan

Tel.: +81-857-31-5240

Fax: +81-857-31-5240

K. Ichino

corresponding author

E-mail: ichino@eecs.tottori-u.ac.jp

results, it seems that the ZnMgSTe quaternary alloy with appropriate composition possesses both a wide bandgap and p-type conductivity.

Keywords ZnMgSTe · ZnS · p-type · wide bandgap · molecular beam epitaxy

PACS 71.20.Nr · 73.61.Ga · 78.40.Fy · 78.55.Et · 81.05.Dz · 81.15.Hi

1 Introduction

A wide bandgap semiconductor ZnS (Eg = 3.7 eV at room temperature) has been known to be difficult to convert into p-type. One of the affecting factors seems to be its low valence band maximum (VBM) energy as shown in Fig. 1, since resulting high hole energy, or low Fermi level can cause various compensations. The VBM of ZnTe, meanwhile, is known to be higher than that of ZnS. Thus substituting a part of S in ZnS with Te causes VBM to move upward and seems to make p-type conversion easier. Actually, we have previously reported p-type conduction in $ZnS_{1-x}Te_x$:N layers in the range of $0.1 < x < 0.3$, and the operation of pn-junction light-emitting diodes [1,2]. With the addition of Te into ZnS, however, the bandgap decreases. On the other hand, with the incorporation of Mg into ZnS or ZnSTe, the bandgap is expected to increase, in which the main contribution is an upward shift of the conduction band minimum. In a ZnMgSTe quaternary alloy, therefore, a large bandgap and p-type conduction seem to be compatible. To date, there have been only a limited number of reports on the growth of ZnMgSTe [3], and thus basic growth conditions of ZnMgSTe should be established first. In this study, we have investigated the growth conditions of ZnMgSTe quaternary alloy layers by molecular beam epitaxy (MBE). We have also carried out p-type doping experiments to study the feasibility of the material.

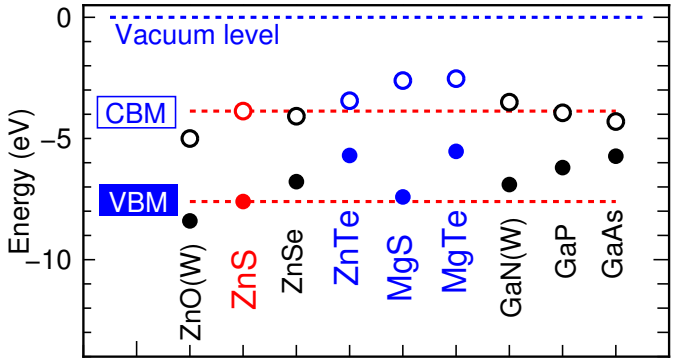

Fig. 1 Valence band maximum (VBM) and conduction band minimum (CBM) of several semiconductors. Note the lowest VBM of ZnS among zincblende-structured semiconductors (see Ref. [1] and references therein).

2 Experimental procedures

ZnMgSTe layers were grown by a MBE system designed for sulfide growth [4,5] using metal Zn, Te (Osaka Asahi Metal), and Mg (Furuuchi Chemical), and elemental S (Furukawa Denshi) as source materials. In this system, ZnS is usually grown at a substrate temperature of 275°C under S-rich condition, in which S source temperature is 155°C and S/Zn flux ratio is estimated to be ∼50. If Te flux is supplied to the S-rich condition, Te is hardly incorporated; even a high Te/S flux ratio of ∼0.2 results in a small Te content y less than 0.01. This is probably because the larger bonding energy of Zn-S than that of Zn-Te is emphasized in S-rich, or Zn-poor condition. On the other hand, when S source temperature is decreased to 110°C, corresponding to a reduction in S flux by approximately one order of magnitude, Te content y is found to be nearly proportional to Te flux, e.g., a Te/S flux ratio of ∼0.06 gives y ∼0.3. These growth conditions had been obtained in our previous study on ZnSTe ternary alloy growth [1,2], and were also used in this study. Composition of the grown films

was evaluated by electron probe micro-analysis (EPMA). As a substrate, a S-doped n-type (001) GaP substrate (Shin-Etsu Handotai) was used. p-type doping was performed using nitrogen (N_2) gas plasma as an acceptor source, supplied from an rf-plasma cell (EIKO ER-1000), typically under the condition of a flow rate of 2.0 sccm and an RF power of 300W. The layers were characterized by high-resolution X-ray diffraction (HRXRD) using Rigaku SmartLab. In the HRXRD measurement, reciprocal space maps (RSMs) around 224 reciprocal lattice points of $Zn_{1-x}Mg_xS_{1-y}Te_y$ and GaP were measured using a Ge-(400) double-crystal monochromator and a 1-dimensional semiconductor array detector (D/teX Ultra). In the photoluminescence (PL) and PL excitation (PLE) spectra measurement, a Xe lamp was used as an excitation light source in combination with a monochromator. Both PL and PLE spectra were recorded at 10 K. Reflectance spectra were recorded using a spectrometer (JASCO V-730) at room temperature (RT).

3 Results and discussion

As already mentioned, the growth of ZnMgSTe quaternary alloy has rarely been reported before. Thus we first investigated basic growth conditions of ZnMgSTe. Since $ZnS_{0.94}Te_{0.06}$ and $Zn_{0.80}Mg_{0.20}S$ are lattice-matched to GaP, ZnMgSTe layers with compositions between them were grown on GaP substrates as a first step. Figure 2 shows a XRD RSM of a $Zn_{0.93}Mg_{0.07}S_{0.96}Te_{0.04}$ layer grown on a GaP (001) substrate with a thin undoped-ZnS buffer layer ($\sim$ 20 nm) inserted in between. The RSM displays the area around the 224 diffraction peaks. The ZnMgSTe layer is nearly lattice-matched, but slightly mismatched to the substrate, as indicated by small dif-

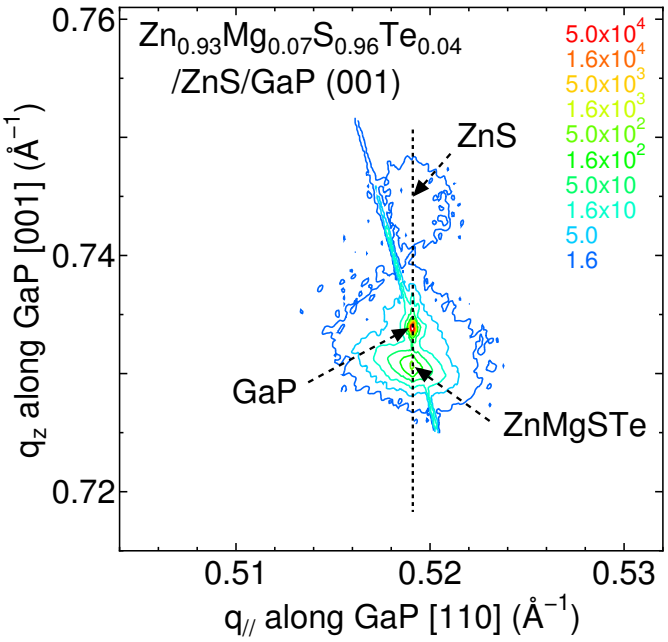

Fig. 2 XRD RSM of $Zn_{0.93}Te_{0.07}S_{0.96}Te_{0.04}$ (180 nm) / ZnS (20 nm) / GaP structure. $q_{//}$ coordinates of the peaks is identical, indicating coherent growth.

ference in the peak position from the GaP peak. The fact that $q_{//}$ coordinate of the ZnMgSTe peak as well as ZnS peak is identical to that of GaP peak shows that the layer is coherently grown onto the substrate. As expected, the ZnMgSTe peak width is rather small, showing high crystalline quality of the ZnMgSTe layer. The full-width at half maximum of the ω-scan rocking curve of the ZnMgSTe 004 peak (not shown) is 260 arcsec, which corresponds to the width of 224 peak in Fig. 2 along ω-scan direction, i.e., along the circle centered at the origin. Based on the growth condition of this sample, ZnMgSTe layers with wider composition range were grown.

In order to study the variation of the bandgap of ZnMgSTe, optical properties of the layers were characterized. Figure 3 shows a reflectance spectrum, as well as PL

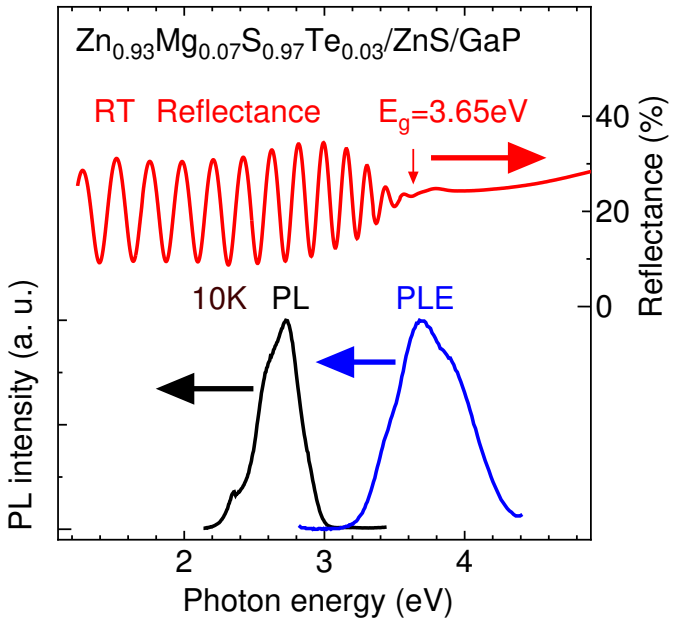

Fig. 3 Reflectance (RT), PL and PLE (10K) spectra of $Zn_{0.93}Mg_{0.07}S_{0.97}Te_{0.03}$/ZnS/GaP structure. The onset of the interference in the reflectance spectrum is taken as the bandgap.

and PLE spectra, of a $Zn_{0.93}Mg_{0.07}S_{0.97}Te_{0.03}$ layer on a GaP substrate. A Te atom in ZnS crystal is known to act as an isoelectronic impurity and causes strong emission below the bandgap under photo-excitation [6,7]. Similarly, Te-containing ZnMgSTe layers exhibit rather strong Te-related PL. To estimate the bandgap, however, PL/PLE spectra are not adequate because PL energy is well below the bandgap due to the nature of the Te trap [8,9], and PLE is also affected by the Te-related states extending below bandgap. Therefore, we used reflectance spectra in this study, and the onset of the interference is simply taken as the bandgap. Although each bandgap thus determined may contain some offset, relative differences in the bandgap can be discussed. If a ZnMgSTe layer is too thin, it is difficult to determine the onset because of the long period of the interference. Thus the layers thicker than $\sim$500nm were used. A

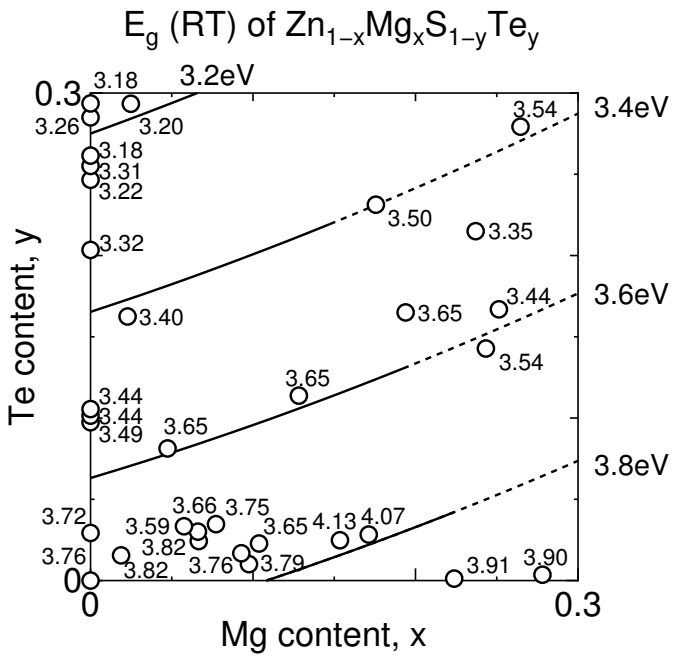

Fig. 4 Experimentally determined bandgaps from reflectance spectra in the area $0 < x, y < 0.3$ of $Zn_{1-x}Mg_xS_{1-y}Te_y$. Each number beside the symbol represents the bandgap for the composition. The lines are to guide the reader's eyes and represent bandgap contours.

ZnS buffer layer is thin and is located under a thick ZnMgSTe layer, and thus it seems to have little effect on the reflectance spectrum. In fact, a bandgap higher than that of ZnS (~ 3.7 eV) can be determined as shown in Fig. 4.

Bandgaps thus estimated for $Zn_{1-x}Mg_xS_{1-y}Te_y$ layers with various compositions x and y are summarized in Fig. 4 showing the area $0 < x, y < 0.3$. Although there seem to be deviations in the values, the bandgap increases with increasing the Mg content, while it decreases with increasing the Te content. The bandgap bowing parameter along y axis indicated by Fig. 4 (~ 1 eV or less) is smaller than the reported values of 1.6-3.8 eV for $ZnS_{1-y}Te_y$ (see Ref. [9] and references therein). This discrepancy

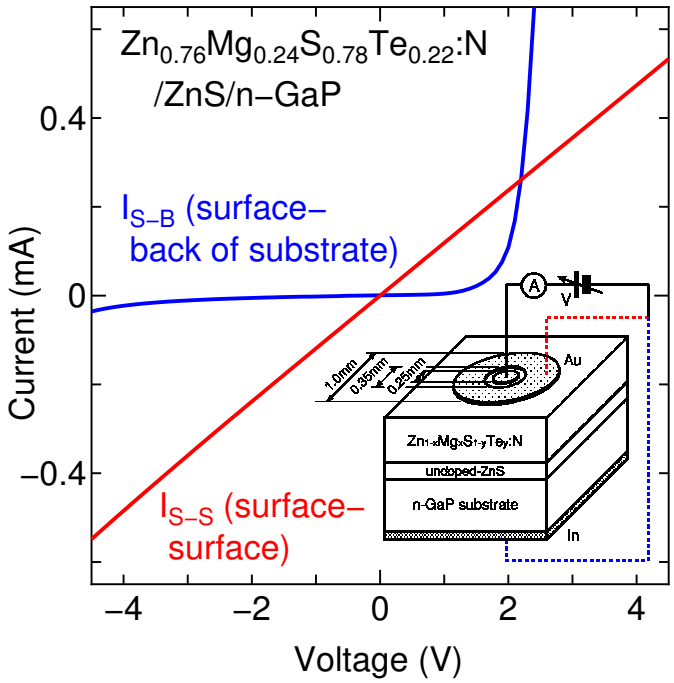

Fig. 5 $I-V$ characteristics of a $Zn_{0.78}Mg_{0.22}S_{0.76}Te_{0.24}$:N layer on a n-GaP substrate. The current was measured in two configurations, surface-surface (I_{S-S}; red line) and surface-the back of the substrate (I_{S-B}; blue line). The inset shows the schematic configuration.

seems to be due to, at least in part, the different effects of Te-related levels in the bandgap. Reflectance spectra seem to be less affected by the Te-related levels compared with absorption spectra, and thus the obtained bandgaps tend to be larger than the values from absorption measurement. Rather large scattering in the bandgaps may be due to the different extent of the effect of Te-related absorption in the bandgap, as well as errors in determining quaternary alloy composition.

For examining the possibility for conduction control, particularly for p-type, electrical properties of the N-acceptor-doped layers were investigated. Figure 5 shows current-voltage ($I-V$) characteristics of a $Zn_{0.78}Mg_{0.22}S_{0.76}Te_{0.24}$:N layer measured

in two different configurations schematically shown in the inset. The current I_{S-S} between the surface contacts (red line) is found to be proportional to the voltage, showing clear ohmic behavior. In addition, since I_{S-S} is larger than the current I_{S-B} between the surface contact and the substrate-back contact in the low voltage range, I_{S-S} is shown to flow within the ZnMgSTe:N layer. In addition, rectification for I_{S-B} for the sample on n-GaP suggests p-type conduction in the ZnMgSTe:N layer. This type of $I-V$ characteristics are often observed for p-type ZnSTe layers. Therefore, the above results indicate ZnMgSTe quaternary alloy crystals have p-type conductivity, as in the case of ZnSTe. In Fig. 5, the starting voltage for current flow, which should be similar to the built-in potential, is smaller than the experimentally determined bandgap of 3.35 eV. For a p-n heterojunction with a small conduction band offset, as in the case of p-ZnS/n-GaP, the built-in potential is roughly equal to the bandgap of p-type material. In the case of p-ZnMgSTe, however, both conduction and valence bands shift upward compared with ZnS as mentioned in the introduction, and thus the built-in potential in p-ZnMgSTe/n-GaP should be roughly equal to $E_{g,\mathrm{ZnMgSTe}} - \Delta E_c$, i.e., the difference between the bandgap of p-ZnMgSTe and the conduction-band offset. In the $Zn_{0.78}Mg_{0.22}S_{0.76}Te_{0.24}$/GaP heterostructure, ΔE_c is roughly estimated to be 0.5 eV, and thus the starting voltage less than 3 V can be explained, at least qualitatively. We have also tried, but failed to determine the carrier type by Hall effect measurement, probably due to a low Hall voltage and a high background voltage, caused by a high carrier concentration and a high resistivity, respectively, as a consequence of a low mobility. A high carrier concentration is also suggested by the fact that Au contacts are ohmic, probably resulting from tunneling.

Owing to the difficulty in obtaining Schottky contact, the determination of acceptor concentration by capacitance-voltage characteristics has not been successful.

Resistivities of the N-doped ZnMgSTe layers were estimated from the $I-V$ characteristics. Here, the resistivity is simply derived from the resistance in two-terminal $I-V$ characteristic taking account of the volume between the contacts. Therefore, contact resistance cannot be excluded, and thus the resultant resistivity value may be overestimated. Figure 6 summarizes the results showing the relation between resistivity and a Te content. It seem that the resistivities of both ZnMgSTe (represented by filled symbols) and ZnSTe (open symbols) similarly depend on the Te content; they decrease with increasing it, although there are rather large deviations. Here, the Mg content in each ZnMgSTe sample is not constant but random, which suggests that the resistivity does not depend on the Mg content. These results seem to support the hypothesis that the valence-band edge energy determines the p-type doping limit. Thus, the results obtained in this study indicate that $Zn_{1-x}Mg_xS_{1-y}Te_y$ quaternary alloy can have similar p-type resistivity and larger bandgap compared with $ZnS_{1-y}Te_y$ ternary alloy with the same Te content.

4 Conclusions

ZnMgSTe quaternary alloy layers have been grown by MBE with the aim of realizing both p-type conduction and a wide bandgap. The quaternary layers nearly lattice-matched to GaP substrates exhibit high crystalline quality. The bandgap, obtained from reflectance spectra, increases with increasing Mg content. *I*-*V* characteristics of N-acceptor-doped ZnMgSTe suggest that the layer is p-type. It was also found that

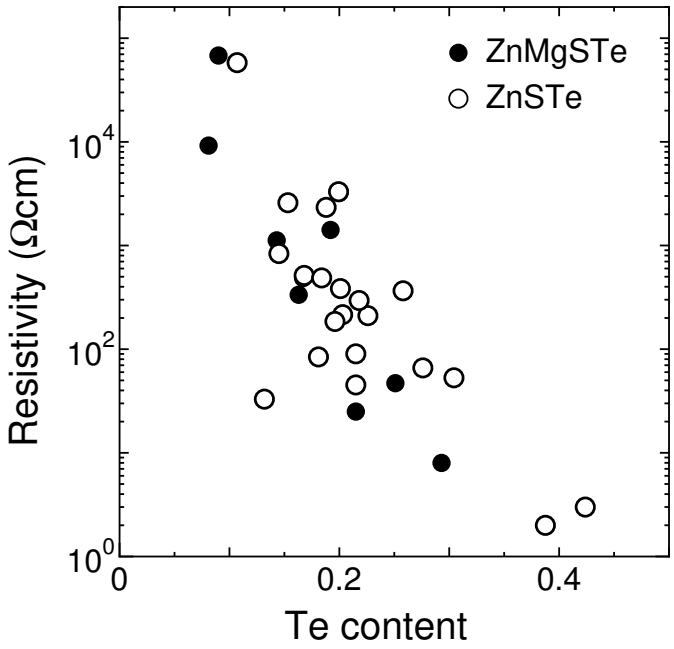

Fig. 6 Resistivity vs. Te content for ZnMgSTe (filled symbols) and ZnSTe (open symbols). Mg content in ZnMgSTe is random.

the resistivity depends on the Te content; it decreases with increasing Te content as in the case of ZnSTe ternary alloy. These results suggest that ZnMgSTe with appropriate composition can have both a large bandgap and p-type conductivity.

Acknowledgements This work was supported in part by JSPS KAKENHI Grant Number 26390053.

References

1. K. Ichino, T. Kojima, S. Obata, T. Kuroyanagi, K. Kimata, S. Nakazawa, and S. Kashiyama, Phys. Status Solidi C 11, 1282, (2014).
2. K. Ichino, T. Kojima, S. Obata, T. Kuroyanagi, S. Nakazawa, and S. Kashiyama, Appl. Phys. Express, 6, 112102, (2013).

3. M. Kobayashi, C. Setiagung, K. Wakao, S. Nakamura, A. Yoshikawa, and K. Takahashi, J. Cryst. Growth 184/185, 66, (1998).
4. K. Ichino, K. Ueyama, M. Yamamoto, H. Kariya, H. Miyata, H. Misasa, M. Kitagawa, and H. Kobayashi, J. Appl. Phys. **87**, 4249 (2000).
5. K. Ichino, T. Nishikawa, F. Kawakami, T. Kosugi, M. Kitagawa, and H. Kobayashi, Phys. Status Solidi B **229**, 217 (2002).
6. G. W. Iseler and A. J. Strauss, J. Lumin. **3**, 1 (1970).
7. I. K. Sou, K. S. Wong, Z. Y. Yang, H. Wang, and G. K. L. Wong, Appl. Phys. Lett. **66** (1995) 1915.
8. T. Fukushima and S. Shionoya, Jpn. J. Appl. Phys. **12**, 549 (1973).
9. Y. Yu, S. Nam, B. O, K. Lee, Y. D. Choi, J. Lee, and P. Y. Yu, Appl. Surf. Sci. **182**, 159 (2001).